



You may also like

Compaction dynamics of a granular medium under vertical tapping

To cite this article: P. Philippe and D. Bideau 2002 *EPL* **60** 677

View the [article online](#) for updates and enhancements.

- [Optical Fiber Sensors Vol III: Components and Subsystems](#)
Peter Cockshott
- [Modeling Volume Change of Large Format Pouch Cells Due to Intercalation](#)
Drew Joseph Pereira, Miguel Fernandez, Kathryn Corine Streng et al.
- [Developments in Mechano-Electrochemical Modeling Methods for Battery Electric Vehicles](#)
Drew Joseph Pereira, Miguel Fernandez, Kathryn Streng et al.

Compaction dynamics of a granular medium under vertical tapping

P. PHILIPPE and D. BIDEAU

*GMCM, Bât. 11A, Campus de Beaulieu, Université de Rennes I
35042 Rennes, France*

(received 5 April 2002; accepted in final form 19 September 2002)

PACS. 45.70.-n – Granular systems.

PACS. 45.70.Cc – Static sandpiles; granular compaction.

PACS. 81.05.Rm – Porous materials; granular materials.

Abstract. – We report new experimental results on granular compaction under consecutive vertical taps. The evolution of the mean volume fraction and of the mean potential energy of a granular packing presents a slow densification until a final steady state, and is reminiscent of usual relaxation in glasses via a stretched exponential law. The intensity of the taps seems to rule the characteristic time of the relaxation according to an Arrhenius’s type relation. Finally, the analysis of the vertical volume fraction profile reveals an almost homogeneous densification in the packing.

Introduction. – Granular matter is a well-known example of athermal systems, that is systems where classical thermodynamics does not apply since thermal energy ($k_B T$) is insignificant compared to the gravitational energy of a macroscopic grain. A static packing of grains is therefore in a metastable state, indefinitely trapped in a local minimum of the total potential energy. When submitted to an external perturbation, the system instantaneously acquires an extra mechanical energy and then relaxes to a new metastable configuration, which depends on the previous one as well as on the nature of the perturbation. This dependence can be investigated by implementing at regular intervals identical external excitations on an assembly of grains and analyzing the succession of static metastable states explored by the system. This is a common experiment in pharmaceuticals when compacting powders but it is also a practical way to “thermalise” a granular medium and to test the conceptual connection between granular compaction and the very slow relaxations of out-of-equilibrium thermal systems [1,2].

The first experiments in this spirit have been carried out in Chicago [3–5]. Starting from a loose packing of beads confined in a tube, a succession of vertical taps of controlled acceleration induces a progressive and very slow compaction of the system. This evolution is well fitted by the inverse of the logarithm of the number of taps and, after more than 10000 taps, a hypothetic steady state is not reached yet. These results have motivated many theoretical and numerical works, most of them dealing with the notion of free volume and geometric constraint [6–8]. Some of them underscore structural aging effects, as currently noticed in glasses.

In this paper, we present new compaction experiments in what we believe to be more general conditions. Indeed, the previous experiences [3–5] were realized in a thin cylinder of diameter $D = 1.88$ cm filled with monodisperse glass spheres of diameter $d = 1, 2$, or 3 mm, that is to say a horizontal gap of 10 to 20 beads ($N_h \sim 10$) between the lateral walls. This condition allows a local measurement of the volume fraction with a capacitive method and prevents any convection in the packing. But, in return, the boundary effects are very strong and may be in particular responsible for the highest values of the volume fraction obtained in some Chicago experiments [4], significantly above the random close-packing limit (approximately 64%) which corresponds to the maximal volume fraction in a disordered packing of identical hard spheres.

Experimental setup. – Our experimental setup is the following: a glass cylinder of diameter 10 cm, filled with 1 mm diameter glass beads on about 10 cm height, is shaken at regular intervals ($\Delta t = 1$ s) by an electromagnetic exciter delivering vertical taps, each of them consisting of an entire cycle of a sine wave (frequency $f = 30$ Hz). The negative peak acceleration a_{\max} felt by the whole system is measured by an accelerometer at the bottom of the cylinder so as to parametrize the tap intensity by the dimensionless acceleration $\Gamma = a_{\max}/g$. By measuring the absorption of a γ -ray beam through the packing, it is possible to estimate the average volume fraction in the bulk $\langle \Phi \rangle$ as well as the vertical density profile $\Phi(z)$, providing a local analysis of the packing structure. We can also deduce the mean potential energy of the heap: $\langle Z \rangle = \int_0^\infty z \Phi(z) dz / \int_0^\infty \Phi(z) dz$.

To restrict the boundary effects, we use here a large horizontal gap ($N_h \sim 100$) even if, therefore, we allow convection to occur during the compaction of the beads, giving rise in particular to an instability of the horizontal free surface [9]. In comparison with the previous experiments [3–5], another important difference concerns the vertical pressure in the static packing: in the narrow tube used in the Chicago’s setup, the pressure felt by the heap at a given height does not correspond to the total weight of the upper packing; part of this weight is screened by the lateral walls (“Janssen effects”). As a consequence, in a static configuration, the vertical pressure is homogeneous in almost all the packing whereas, here, the vertical pressure is definitely not saturated in the packing but probably close to the hydrostatic pressure. Nevertheless, we do not know to what extent the initial static situation can play a role in the dynamical process induced by a tap.

The measure is deduced from the transmission ratio of the horizontal collimated γ beam through the packing: $T = A/A_0$, where A and A_0 are, respectively, the activities counted on the detector with and without the presence of the beads in the cylinder. From the Beer-Lambert’s law for absorption, we can derive an estimation of the volume fraction in the probe zone: $\Phi \approx -(\mu D)^{-1} \ln(T)$. Here μ is the absorption coefficient of the beads; it was evaluated experimentally to $\mu \approx 0.188 \text{ cm}^{-1}$ for our γ beam of energy 662 keV (^{137}Cs source).

The collimated γ beam is nearly cylindrical with a diameter of 10 mm and intercepts perpendicularly the vertical axis of the cylinder of beads. An acquisition time of 60 seconds for each measure was found as a good consensus between the intrinsic uncertainty of the radioactive beam and the total duration of an experiment. We then achieve a precision $\Delta \Phi \approx 0.003$. Two types of measurement are used: vertical profile $\Phi(z)$ and mean volume fraction $\langle \Phi \rangle$. The vertical volume fraction profile is deduced from 63 measures of the γ -transmission at successive heights z with a regular step $\Delta z \approx 2$ mm; each measure is an average on a horizontal slice obtained by 1 turn rotation of the cylinder about its axis during the measure. $\langle \Phi \rangle$ is estimated from the transmission ratio T averaged on approximately 7 cm height from the bottom of the cylinder: the cylinder achieves a vertical translation of 7 cm combined with a rotation of 2 turns so as to permit a significant saving of time. With the aim of

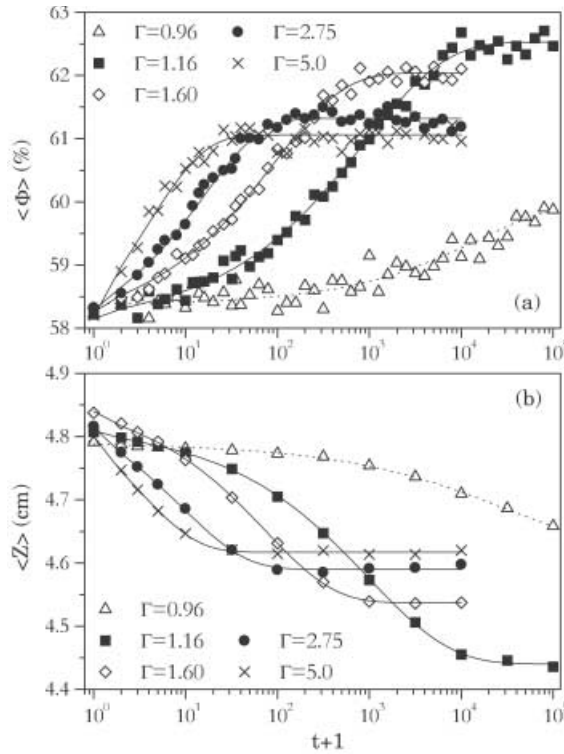


Fig. 1 – (a) Temporal evolution of the mean volume fraction $\langle \Phi \rangle$ for different tapping intensities Γ : $\Gamma = 0.96$ (\triangle), $\Gamma = 1.16$ (\blacksquare), $\Gamma = 1.60$ (\diamond), $\Gamma = 2.75$ (\bullet), and $\Gamma = 5.0$ (\times). (b) Temporal evolution of the mean potential energy $\langle Z \rangle$ for the same values of Γ . To make the curves easier to examine, only an approximate 25% of the experimental points of the mean volume fraction are plotted.

limiting the duration of the experiments and of avoiding redundant information due to the very slow evolution of the system, the measurements are spaced out in time (on a logarithmic scale) with 2 measures of profile and 50 measures of $\langle \Phi \rangle$ per decade (except 10 for the first decade).

Compaction dynamics. – Several compaction experiments were carried out for different values of the tapping strength Γ in the range $[0, 6]$. Part of the results are presented in fig. 1 which shows the evolution of the mean volume fraction $\langle \Phi \rangle$ and of the mean potential energy $\langle Z \rangle$ during 10000 or 100000 taps and for a few values of Γ . These curves are either raw data or an average on 2 or 3 realizations. Here we call “time”, t , the number of taps and the “dynamics” is the succession of static equilibrium induced by the taps. $\langle \Phi \rangle$ and $\langle Z \rangle$ are plotted *vs.* $\log(t+1)$ as a convenient way to include the initial state ($t = 0$) on the logarithmic axis. This initial state corresponds to a loose packing ($\langle \Phi \rangle = 58.3 \pm 0.3\%$) prepared in a reproducible way.

The typical evolution is a slow compaction of the packing characterized by an increase of $\langle \Phi \rangle$ and a reciprocal decrease of $\langle Z \rangle$. Then, after a varying relaxation time, the system finally reaches a steady state. Note that for $\Gamma = 0.96$, the temporal window accessible in the experiments becomes too small to observe the whole relaxation process; but a compaction obviously occurs although Γ is smaller than the “dynamical” threshold Γ^* ($\Gamma^* \approx 1.2$) above which there is a collective takeoff of the packing from the bottom of the cylinder. When

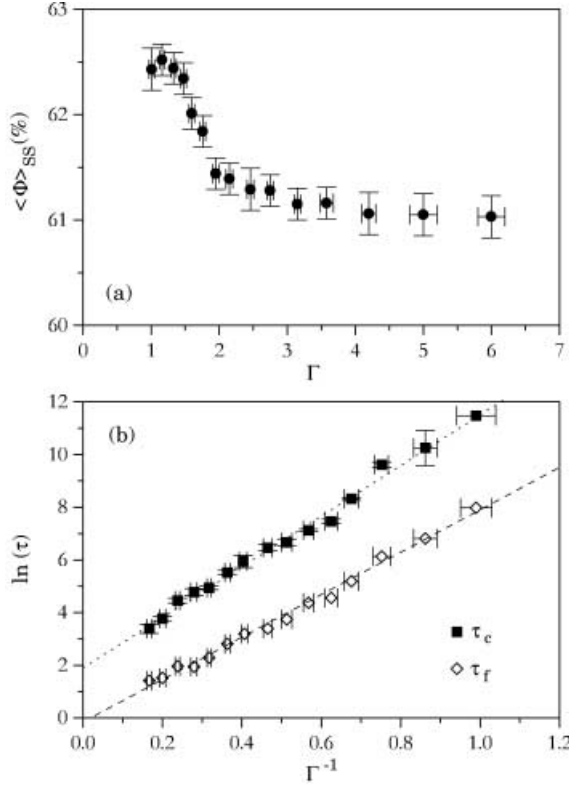


Fig. 2 – (a) Volume fraction of the steady state $\langle \Phi \rangle_{ss}$ vs. Γ . (b) The experimental estimation of the relaxation time τ_c (■) and the characteristic time τ_f (◇) of the stretched exponential fit as functions of the inverse of the tapping intensity Γ (τ_c and τ_f are defined in the text). The lines are linear fits corresponding to Arrhenius laws (see eq. (3)).

reached, the final steady state is all the more compact (*i.e.* small value of $\langle Z \rangle_{ss}$ and high value of $\langle \Phi \rangle_{ss}$) as the tapping strength is slight (see fig. 2a); but, in return, the number of taps needed increases significantly. In all our experiences, the volume fraction stays below the random close-packing limit which tends to reject any hypothesis of ordering or crystallization in the packing. Convection seems also to play a role in the compaction process: in fig. 2a, we observe indeed a significant change in the dependence of $\langle \Phi \rangle_{ss}$ on Γ which might correspond to different convective regimes. Under a threshold $\Gamma_c \approx 2$, the final state of the free surface of the packing is an inclined plane and indicates a spontaneous breaking of symmetry. Above Γ_c , the free surface heaps up moderately and finally takes a flat conical shape probably brought about by a nearly torical convective roll. These sorts of free surface instabilities have already been observed, see, for instance, [9].

In comparison with the previous experimental results [3], some sharp differences appear. First, the shapes of the compaction curves differ significantly, especially concerning the long-time behavior and the obtaining of a final steady state which is here definitely established and may correspond to a dynamical balance between compaction and convection. Moreover, for a given intensity Γ , the dynamics of the compaction seems slower in the Chicago's experiments, particularly for the highest values of Γ . We believe that these differences are principally due to the disparity of the lateral constraint (horizontal gap N_h) in the two configurations ($N_h \sim 10$

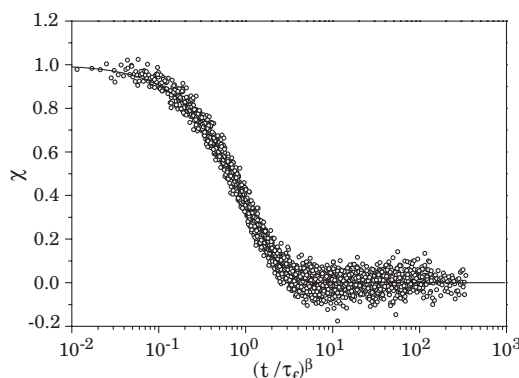


Fig. 3 – Collapse of the compaction curves obtained with $\Gamma = 1.01, 1.16, 1.33, 1.48, 1.60, 1.76, 1.95, 2.15, 2.46, 2.75, 3.15, 3.58, 4.20, 5.0$, and 6.0 : $\chi = (\langle\Phi\rangle_{ss} - \langle\Phi\rangle(t)) / (\langle\Phi\rangle_{ss} - \langle\Phi\rangle(0))$ is plotted *vs.* $(t/\tau_f)^\beta$. The solid line is the function $f(u) = \exp[-u]$ corresponding to the stretched exponential law.

against $N_h \sim 100$). To extend the comparison, we have tried to fit $\langle\Phi\rangle$ with the empirical law initially proposed in [3]:

$$\langle\Phi\rangle(t) = \langle\Phi\rangle_\infty - \frac{\Delta\langle\Phi\rangle_\infty}{1 + B \ln(1 + t/\tau)}. \quad (1)$$

The result is satisfactory concerning the beginning of a typical compaction curve but fails to correctly fit the final relaxation up to the steady state. In particular, the parameter $\langle\Phi\rangle_\infty$ sharply overestimates the steady-state volume fraction $\langle\Phi\rangle_{ss}$ at small Γ . On the contrary, our data concerning $\langle\Phi\rangle$ as well as $\langle Z\rangle$ are in very good agreement with a stretched exponential function (eq. (2)) on the whole temporal range. First used by Kohlrausch in 1854 [10], this expression was far later popularized by Williams and Watts [11]. It is now frequently applied to a large range of relaxations in disordered thermal systems as glasses (see, for example, [12] and references therein) and is often called KWW law,

$$X(t) = X_\infty - (X_\infty - X_0) \exp \left[- (t/\tau_f)^\beta \right] \quad \text{with } X = \langle\Phi\rangle \text{ or } \langle Z\rangle. \quad (2)$$

As X_∞ can be approximated by X_{ss} and X_0 by $X(t=0)$, eq. (2) has only two free parameters (τ_f and β). Examples of this fit are presented in fig. 1, where the solid lines are the stretched exponential laws. For $\Gamma = 0.96$ and, more generally, for $\Gamma \lesssim 1$, only the beginning of the relaxation is accessible and there is so no evidence that a stretched exponential law still describes the compaction dynamics; consequently, the corresponding fit is plotted in the dotted line. The values obtained for β are in the range 0.5–0.8 and tend to increase slightly with Γ , whereas τ_f decreases strongly with Γ .

A general collapse of the compaction curves can be obtained by use of the function χ , defined as the rate of increase of $\langle\Phi\rangle$: $\chi(t) = (\langle\Phi\rangle_{ss} - \langle\Phi\rangle(t)) / (\langle\Phi\rangle_{ss} - \langle\Phi\rangle(0)) = f((t/\tau_f)^\beta)$. Figure 3 presents the plot of χ *vs.* $(t/\tau_f)^\beta$; the solid line plots the KWW fit. The fluctuations at large t correspond to the final steady state and are particularly significant at large Γ .

Relaxation time. – To quantify more precisely the influence of Γ on the dynamics of the compaction, it is possible to estimate a characteristic relaxation time. To do this, we use two different initial packings: the loose one, already presented above ($\langle\Phi\rangle = 58.3 \pm 0.3\%$), and a more compact one ($\langle\Phi\rangle = 63.2 \pm 0.2\%$). Submitted to identical taps, the first packing densifies whereas the other dilates and both of them progressively meet, reaching the same

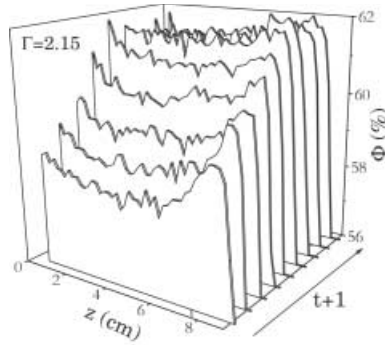


Fig. 4 – Quasi-homogeneous compaction of the vertical volume fraction profile. The profiles are represented in the range $56\% < \Phi < 62\%$ and $0 < z < 9$ cm and correspond to the following tap numbers: $t + 1 = 1, 3, 10, 32, 100, 316, 1000, 3.162, \text{ and } 10000$.

steady state. From this meeting point, we can evaluate a time of convergence τ_c . As most of the usual disordered packings of monodisperse beads have a packing fraction comprised between 58.3% and 63.2%, this time can also be regarded as a memory effect and can be interpreted as the number of taps required for a packing to “forget” its initial configuration. When analysing the dependence on Γ of this characteristic time τ_c as well as of the parameter time τ_f of the stretched exponential fit, we found that an Arrhenius behavior (eq. (3)) describes reasonably well the experimental dynamics as illustrated in fig. 2b:

$$\tau_{c,f}(\Gamma) = \tau_0 \exp \left[\frac{\Gamma_0}{\Gamma} \right]. \quad (3)$$

In the two cases, we have obtained ($\Gamma_0 \approx 9.6$, $\tau_0 \approx 6.7$) for τ_c and ($\Gamma_0 \approx 8.0$, $\tau_0 \approx 0.9$) for τ_f .

Finally, we present in fig. 4 a typical evolution of the vertical volume fraction profile in the case of $\Gamma = 2.15$. To observe the progressive densification of the packing, we use a zoom on the zone of interest ($56\% < \Phi < 62\%$) and a three-dimensional representation with the third axis corresponding to time on a logarithmic scale. The profile is plotted approximately every half-decade.

We note that the compaction is rather homogeneous in the bulk; there is no upward or downward densification front. The profile continuously reaches a final steady state. This asymptotic profile is nearly uniform, a slight positive gradient ($d\Phi/dz > 0$) appears for $\Gamma \geq 2$; this observation agrees with previous experimental [3] and numerical [7] results. We have also verified that the same steady-state profile is obtained when starting from the initial dense packing ($\langle \Phi \rangle = 63.2 \pm 0.2\%$) instead of the loose one.

Conclusion and perspectives. – In conclusion, we have shown that, in the case where the lateral constraint is weak, granular compaction by vertical taps is quite similar to a typical relaxation of an out-of-equilibrium thermal system. Indeed, the densification curves can be reasonably well fitted by a stretched exponential or KWW law. The characteristic time of compaction (τ_c or τ_f) follows an Arrhenius relation where the dimensionless acceleration Γ plays the role of temperature. These results confirm and reinforce the analogy between compaction dynamics and “glassy” phenomena. Moreover, the acquisition of the vertical volume fraction profile has established that the compaction is rather homogeneous in all the packing. Further investigations are in progress to study more precisely the influence of the lateral constraint (N_h) and to clarify the link between convection and compaction.

* * *

We are grateful to A. VALANCE and R. DELANNAY for a careful reading of the manuscript, and to S. BOURLES and P. CHASLE for technical assistance.

REFERENCES

- [1] EDWARDS S. F. and OAKESHOTT R. B. S., *Physica A*, **157** (1989) 1080; MEHTA A. and EDWARDS S. F., *Physica A*, **157** (1989) 1091.
- [2] NICODEMI M., CONIGLIO A. and HERRMANN H. J., *Phys. Rev. E*, **55** (1997) 3962; KURCHAN J., *J. Phys. Condens. Matter*, **12** (2000) 6611.
- [3] KNIGHT J. B., FANDRICH C. G., LAU C. N., JAEGER H. M. and NAGEL S. R., *Phys. Rev. E*, **51** (1995) 3957.
- [4] NOWAK E. R., KNIGHT J. B., POVINELLI M. L., JAEGER H. M. and NAGEL S. R., *Powder Technol.*, **94** (1997) 79.
- [5] NOWAK E. R., KNIGHT J. B., BEN-NAIM E., JAEGER H. M. and NAGEL S. R., *Phys. Rev. E*, **57** (1998) 1971.
- [6] BARKER G. C. and MEHTA A., *Phys. Rev. E*, **47** (1993) 184; PHILIPPE P. and BIDEAU D., *Phys. Rev. E*, **63** (2001) 051304.
- [7] BARRAT A. and LORETO V., *J. Phys. A*, **33** (2000) 4401.
- [8] KRAPIVSKY P. L. and BEN-NAIM E., *J. Chem. Phys.*, **100** (1994) 6778.
- [9] EVESQUE P. and RAJCHENBACH J., *Phys. Rev. Lett.*, **62** (1989) 44; LAROCHE C., DOUADY S. and FAUVE S., *J. Phys. (Paris)*, **50** (1989) 699.
- [10] KOHLRAUSCH R., *Pogg. Ann. Phys. Chem.*, **91** (1854) 179.
- [11] WILLIAMS G. and WATTS D. C., *Trans. Faraday Soc.*, **66** (1970) 80.
- [12] PHILLIPS J. C., *Rep. Prog. Phys.*, **59** (1996) 1133.